

1-1-1996

## The Anomalous Behavior of SH-Waves Across the Water Table

P. Michaels  
*Boise State University*

W. Barrash  
*Boise State University*

---

### Publication Information

Michaels, P. and Barrash, W. (1996). "The Anomalous Behavior of SH-Waves Across the Water Table". In *Symposium on the Application of Geophysics to Engineering and Environmental Problems 1996* (pp. 137-145). The Environmental and Engineering Geophysical Society (EEGS). <https://doi.org/10.4133/1.2922266>

This article was originally published by The Environmental and Engineering Geophysical Society (EEGS) in *Symposium on the Application of Geophysics to Engineering and Environmental Problems 1996*. Copyright restrictions may apply. <https://doi.org/10.4133/1.2922266>

# THE ANOMALOUS BEHAVIOR OF SH-WAVES ACROSS THE WATER TABLE

P. Michaels and W. Barrash

Center of Geophysical Investigation of the Shallow Subsurface  
Boise State University  
1910 University Drive  
Boise, Idaho 83725

## ABSTRACT

Most theoretical studies of seismic wave propagation in a porous medium do not predict a significant increase in SH-wave velocity with increasing water saturation. Although that type of behavior is commonly predicted for P-waves (and confirmed by countless observations), the expectation for SH-waves is a slight decrease in propagation velocity with increasing water saturations. While published measurements of SH-wave velocity in laboratory studies have been supportive of such a slight decrease in velocity, the data have been biased towards high pressures (typical of oil reservoirs at large depths of burial). On the other hand, the few published low pressure laboratory measurements have revealed significantly different results.

The authors' in-situ measurements of seismic wave velocities in a shallow, coarse grained, unconfined alluvial aquifer document a significant SH-wave velocity increase in the transition from the vadose zone to the water table. In one vertical seismic profile (VSP), the P-wave velocity increases by a factor of 4.2 and the SH-wave velocity increases by a factor of 2.6. What is not clear at this point is the true nature of the increase. Is the velocity increase an expression of the presence of water in the pores, or does water alter the rigidity of the soil matrix?

In addition to the broad-band velocity increase, we have also observed changes in the attenuation of SH-waves across the water table. After correcting for geometric spreading, the amplitude decay observed in the vadose zone has been found to be larger than that observed below the water table. However, the variation in amplitude decay as a function of frequency and the measurements of body wave dispersion were found to be larger below the water table than above. That is, the water saturated soil behavior is consistent with a Voigt solid, but the dry material appears to follow a different model.

The authors will discuss these observations in the context of the current debate on Poisson's ratio and the  $V_p/V_s$  ratio.

## INTRODUCTION

Engineering geophysicists often work in soils at shallow depths. This zone of interest is characterized by highly variable porosities, permeabilities, water saturations, elastic moduli, and low confining pressures. Consequently, there is a need to understand the behavior of mechanical waves under these varying conditions.

The velocity behavior of mechanical waves as a function of water saturation has been investigated in laboratory studies over the years by researchers which include Domenico (1977) and Gregory (1976). In large part, this work has been supported by the petroleum industry in search of tools to seismically discriminate between the various pore fluids and sedimentary rock types. Often, comparison of results from laboratory studies to predictions from existing theories have been favorable. There have been notable exceptions, however. For example, Gregory (1976) found that not all his tests were in agreement with Biot's (1956) theories for shear waves. Specifically, Gregory's Class II rocks displayed an increase in shear wave velocity as water saturation increased. This stands in contrast to Gregory's Class I rocks which agree with predictions of a slight decrease in shear wave velocity with increasing water saturation. The Class II rocks were characterized by low porosity and were tested at low confining pressures at frequencies of 1 MHz.

Furthermore, a recent article by Gretener (1994) has triggered a debate (Domenico, 1995) over the extension of existing seismic experience to the area of soil mechanics. Given the enormous differences between indurated rocks and noncohesive soils, one might well hesitate to extend experiences from one field to the other (not to mention issues of static vs. dynamic, and linear vs. nonlinear, large strain vs. small strain). For that reason, we

were motivated to begin documenting in-situ seismic measurements of shear waves in soils under variable water saturations at shallow depths of burial.

In particular, we were curious to see if shallow soils followed the more traditional behavior of Gregory's Class I rocks, or the anomalous behavior exhibited by his Class II rocks. One might expect Class II behavior in soils since the confining pressures are much less (even though porosities are generally large). We were also motivated by an omission in Domenico's (1995) Table 2. He omitted the low pressure shear wave data for saturated rock. If one extends the trend in Domenico's data, it appears that shear wave velocities in brine saturated sands could cross-over and exceed velocities of gas saturated sands at low pressures.

## FIELD DATA COLLECTION

We collected our data at a site in downtown Boise, Idaho. Located approximately 0.5 Km from the Boise River, the site is currently being treated for ground water contamination. We were given access to several geotechnical boreholes that had been drilled at the site. Only one borehole (SPT-3) was large enough to be logged with our Mark products 3-component side-wall clamping tool. We did log other narrow holes with a rented tool which employed a pneumatic clamp. We did not recover any useful P-wave data due to the poor clamping in the vertical direction. However, the SH-wave results from these other holes were in good agreement with those from the well presented in this paper.

### Seismic Data Collection

The Mark product tool employs a metal bow-spring which releases at the bottom of the hole. A full waveform vertical seismic profile (VSP) was acquired with both SH- and P-wave sources by pulling the clamped phone up the hole. Stations were recorded at every 0.5 meters. A stationary reference phone monitored each source effort, revealing a highly repeatable waveform. The SH-wave source used horizontal pendulums and was struck on opposite ends to confirm and enhance shear waves by subtraction of opposite polarity source efforts. A vertical pendulum source was used for the P-wave recordings. Both sources involve a sledge hammer pendulum striking a wood surface. We have found that stacking 15 to 20 light blows against wood gives better bandwidth than striking metal base plates which tend to ring at a dominant frequency.

A Bison 9048 engineering seismograph with filters set at 8 to 1000 Hz recorded the data. The sample interval was 0.0002 seconds and a record length of 0.5 seconds was recorded. The geophone elements were 10 Hz phones with 70% damping.

### Site Geology

The system under study at the Boise site is a shallow, unconfined aquifer in Quaternary-Recent coarse, unconsolidated alluvium of the Boise River. The materials at the site, from land surface to the base of the shallow aquifer, can be divided into three units which are:

- Soil and industrial detritus (0 to ~3m)
- Lenses of cobbles and sand (~3m to ~16m)
- Sand and silty sand (~16m to ~20m).

Cobble size ranges from .05 to > 0.2m diameter. Cobble lenses generally have a sand matrix. For lenses or zones within the alluvial (lower two) units, porosity estimates and measurements are in the range of 0.25 to 0.45, and hydraulic conductivity estimates and measurements range from less than .001 to 0.1 cm/s. The water table was in the cobble-and-sand unit, about 5.5m below land surface. This level was measured in December 1994, the same month in which the VSP measurements were taken at well SPT3.

## DATA ANALYSIS

### Evidence Of Class II Behavior

The SH-wave data were taken from the two horizontal components and rotated to align one component parallel to the source axis. The P-wave data were taken from the vertical phone. In all cases, a stationary

reference phone was used to adjust signals from each level to a standard source amplitude.

Figure 1 shows the waveform data for both the SH- and P-wave records. Also shown is a simplified geologic column. The data have been trace equalized before plotting to maintain a visible waveform on all levels. The first step was to pick the broad-band arrival times at each level. For the SH-wave data, the first motion polarity is a positive deflection (black). For the P-wave data, first motion is taken as a negative deflection (white). It should be noted that the very shallow P-wave data (first 3 levels) are dominated by surface wave energy. This is a consequence of the vertical source moment which radiates very little body wave energy in the horizontal direction, and the fact that the vertical phone is polarized at right angles to the main particle motion of a horizontally propagating P-wave, to the extent that it exists.

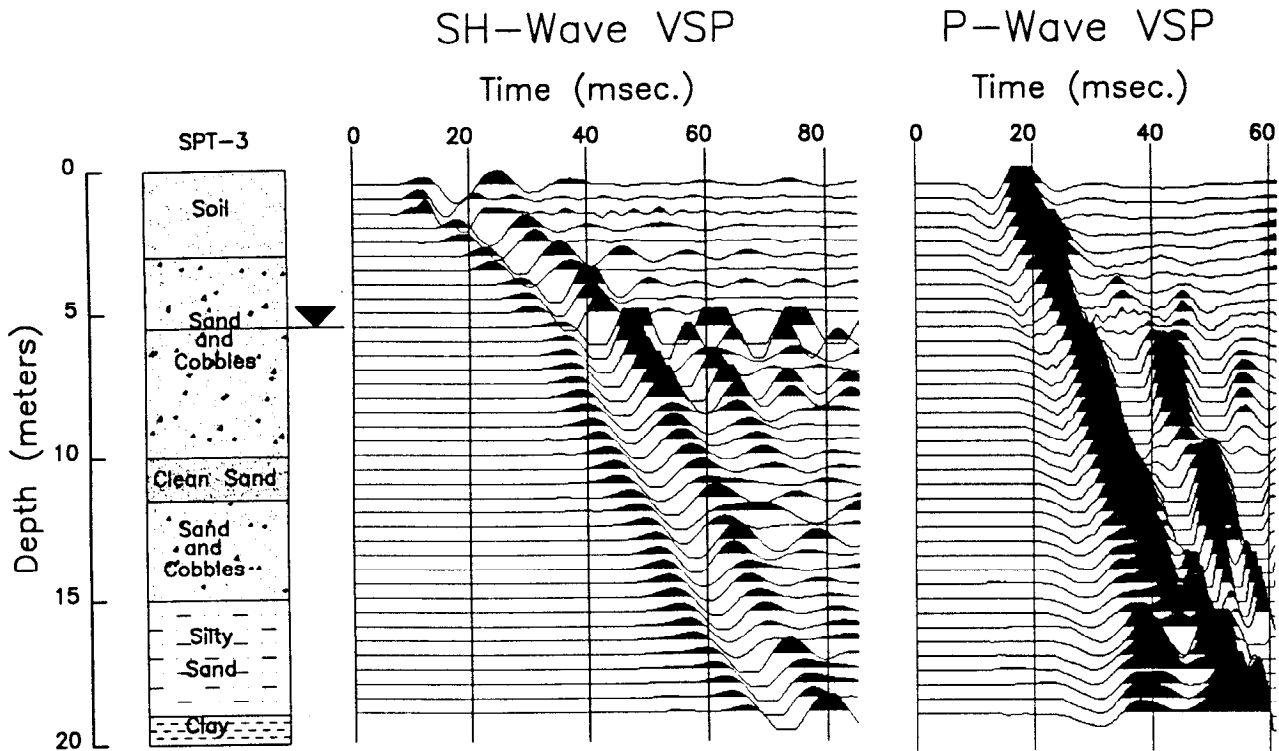
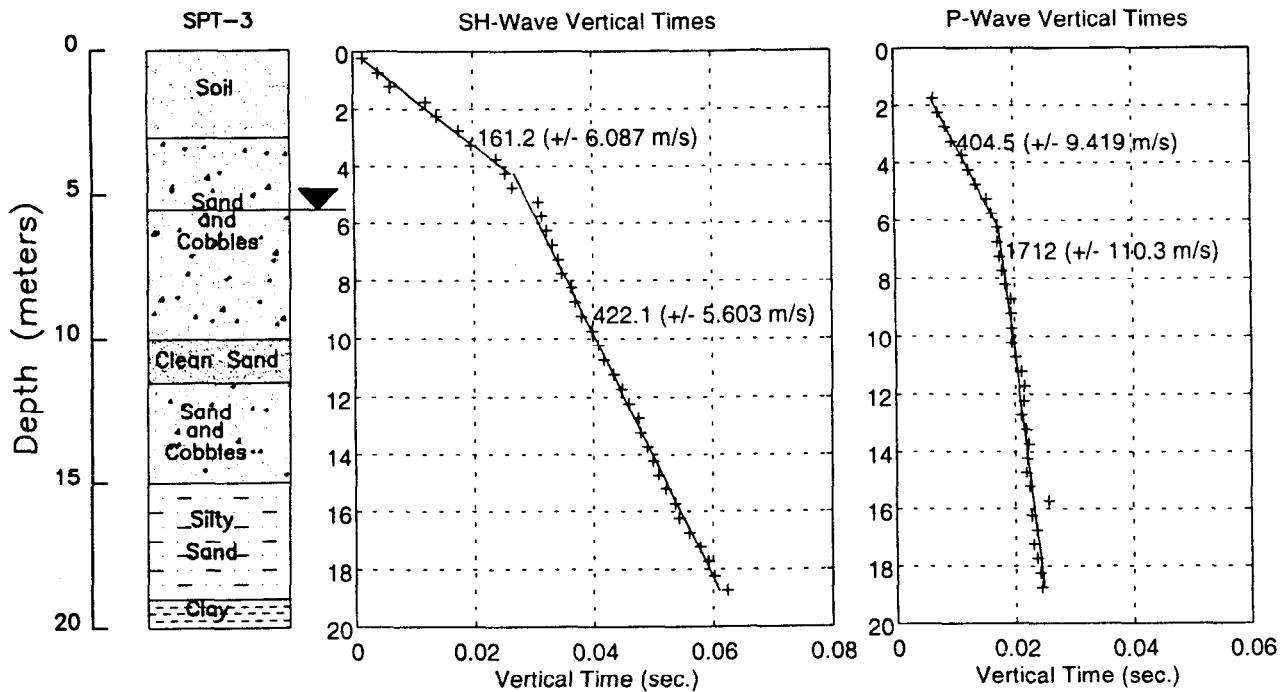


Figure 1. Geologic column and the full waveform VSP first arrival data. The first motion is positive (black) on the SH-wave data. Following the SH-wave enhancement (subtraction of opposite polarity source efforts), the data have been rotated to a horizontal component parallel to the source axis. The first motion on the P-wave data is negative (white). Only the vertical component data are displayed on the P-wave VSP. All signals have been trace equalized to maintain visibility of the waveforms.

Figure 2 shows plots of vertical travel time computed from the picked first arrival times. Vertical time,  $t_v(z)$ , is computed by the cosine projection of the first arrival time,  $t(z)$ ,

$$t_v(z) = t(z) \cdot \frac{z}{\sqrt{x^2 + z^2}}$$

where  $z$  is the geophone depth below the source and  $x$  is the horizontal source offset (1 meter). A major break in the P-wave times occurs at the water table (5.5 meters depth below ground level). The slope of the vertical time plot is used to compute a velocity for each major interval in the soil profile. These velocities are indicated on the plots, along with appropriate error bars. Note that a similar major break in slope occurs on the SH-wave data of Figure 2. However, this break is shallower (at 4 meters depth).



**Figure 2.** Geologic column and vertical time plots for both the SH- and P-wave broad-band VSP data. The first arrival time picks extracted from the data shown in Figure 1 are projected to the vertical in these plots (see text). Note that the SH-wave data has a major break in slope at about 4 meters (top of the partial water saturations). The P-wave data break in slope is deeper (~6m) and corresponds to full water saturation of the available pore space. The vertical times are plotted as "+", and a linear regression of the data for both the shallow and deep intervals is indicated by the solid curves. Soil velocities are computed from the slope of the linear regressions and are labeled with respective error bars.

The hole was also logged with neutron and temperature tools. Figure 3 (A) shows the epithermal neutron log. Note that the neutron counts begin to decrease at 4 meters, and reach a minimum level at 5.5 meters. We interpret the zone from 4 to 5.5 meters as one in which the partial water saturations are increasing with increasing depth. This may be explained either as a capillary fringe, or as a zone of descending recharge due to the rains in November and December. Both the logs and the VSP were acquired in the month of December, 1994. Above 4 meters, the water saturations are very low.

Further support for the neutron interpretation can be found in the temperature log, Figure 3 (B). This log shows that the temperature rose abruptly when the probe encountered water in the bore hole (about 5.5 meters, close to where P-wave velocity increases). Also note that at 4 meters depth, the temperature curve breaks in slope coincident with the break in slope of the SH-wave velocities. This may indicate an increase in thermal conductivity due to increased presence of water in the pores.

From these data, it appears that SH-wave velocities are sensitive to much lower water saturations than P-waves. Since confining pressures are low, this appears to be behavior in soils consistent with Gregory's Type II rocks. However, we hasten to add that these are non-cohesive soils (not rocks), and it is not clear how far this experience can be extended to other geologic settings.

One possible value of SH-wave sensitivity to partial water saturations might be in the mapping and study of recharge in unconfined aquifers. Other applications might be in the mapping of toxic liquid spills within the vadose zone. However, additional observations are needed to determine what role porosity variations might also play in this effect.

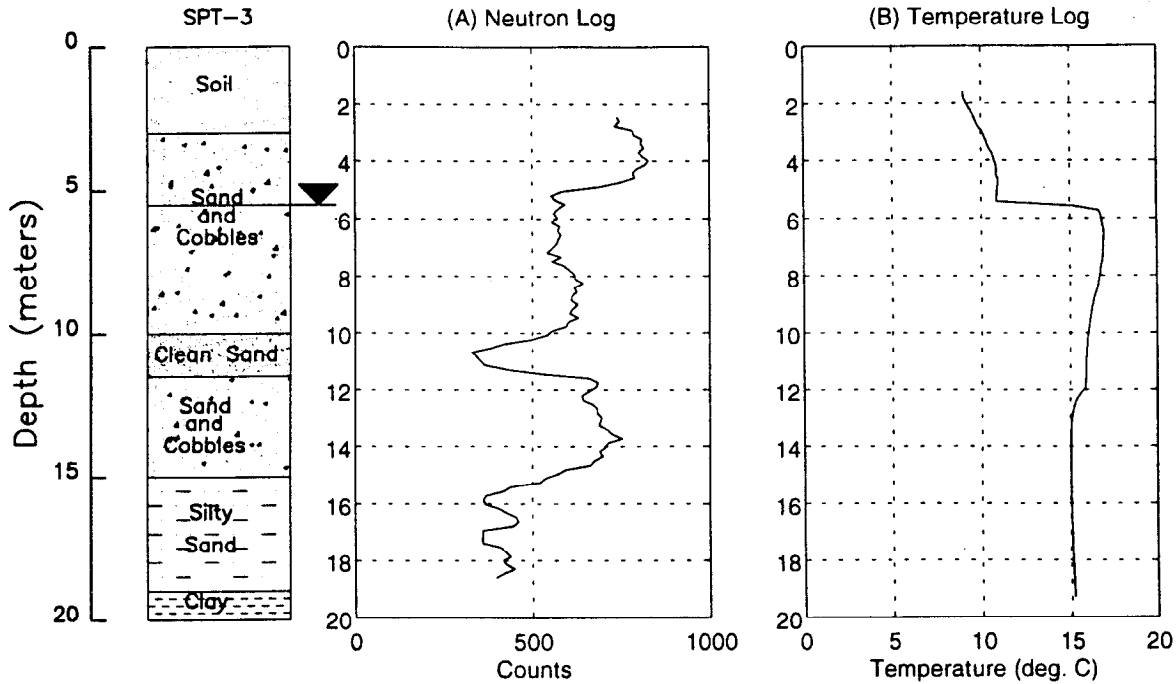


**Figure 3.** Geologic column, (A) epithermal neutron, and (B) temperature logs. Above the water table, the neutron log responds largely to variations in water saturation (low counts corresponding to high water saturation). Below the water table, the neutron log is essentially a porosity tool. We interpret increasing water saturations beginning at 4 m depth, as expressed by the decline in neutron counts. Also, at 4 m depth, the slope on the temperature log decreases, possibly indicating an increase in thermal conductivity due to increased water saturations. The major increase in temperature (5.5 m) indicates the depth at which the temperature probe encountered water in the borehole. The temperature log was acquired at a 5 cm/sec logging rate.

### Inelastic Analysis

Many authors feel that the presence of water in porous media should lead to body wave dispersion. For example, Biot (1962) describes how a viscous fluid between grains can be represented by a dashpot in parallel with a spring. We used this model to study 1-D wave propagation in the VSP experiment. Extending the model to a continuum, the relevant wave equation is

$$\frac{\partial^2 u}{\partial t^2} = C_1 \frac{\partial^2 u}{\partial x^2} + C_2 \frac{\partial^3 u}{\partial x^2 \partial t}$$

where  $u$  is particle velocity induced by the wave,  $C_1$  is an elastic coefficient (spring), and  $C_2$  is the damping coefficient (dashpot). These two coefficients are constant for a medium and are the values which an engineer would use in the stiffness and damping matrices for computation of ground motions during an earthquake. Substitution of the ansatz solution in the form,

$$u(x, t) = \exp(-\alpha x) \cdot \cos(kx - \omega t)$$

leads to the following frequency variant expressions for decay and phase velocity of the wave,

$$\alpha = \frac{4\sqrt{B}\omega^2 C_2}{(2\omega C_2)^2 + B^2} \quad C = \frac{2\omega^2 C_2}{B\alpha}$$

$$B = 2\left[C_1 + \sqrt{C_1^2 + \omega^2 C_2^2}\right]$$

Here  $C$  is phase velocity, and  $\alpha$  is the attenuation coefficient (both functions of frequency,  $\omega$ ). The distance variable is  $x$ , time is given by  $t$ , and wavenumber is  $k$ . The above simplifies to the elastic wave equation when  $C_2$  is set to zero. In that case,  $\alpha$  vanishes and the phase velocity reduces to

$$C = \sqrt{C_1}$$

which is frequency invariant. This model (sometimes known as a Voigt solid) predicts increased decay,  $\alpha$ , and increased phase velocity,  $c$ , as frequency increases. At an intuitive level, the viscosity of the pore waters effectively provide an increased "stiffness", resulting in greater wave speed.

### Measurement of Amplitude Decay

Figure 4 shows our measurements of SH-wave amplitude decay after corrections for spherical divergence. The attenuation coefficient,  $\alpha$ , is plotted for a shallow zone (2.0 to 6.0 meters), (A), and a deeper fully saturated zone (6.0 to 14.0 meters), (B). The shallow zone measurements were difficult to make at high frequencies due to interference from back scatter and reflections. They are unreliable at frequencies above 40 Hz. As can be seen, in the partially saturated shallow soil, we did not observe the expected increase in attenuation coefficient with increasing frequency. However, the deeper, water saturated zone did exhibit the classic behavior of increasing attenuation coefficient with increasing frequency. Presumably, different relaxation mechanisms dominate the two zones. Note that the presence of pore waters actually appears to lessen the attenuation coefficient at low frequencies in comparison to the partially saturated soil.

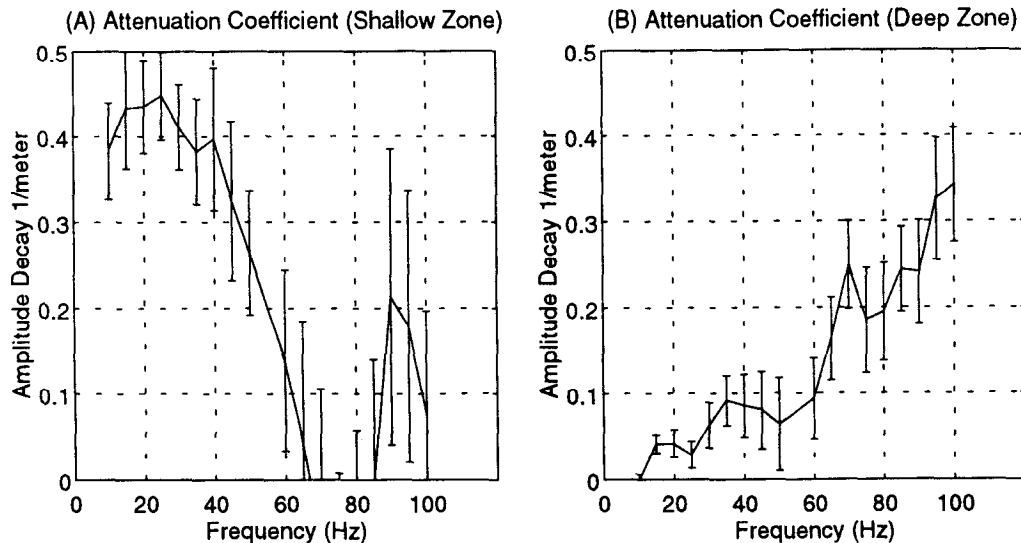


**Figure 4.** Attenuation coefficient measured in the (A) shallow zone and (B) deeper zone (see text). Measurement of decay is extremely difficult in the partially saturated shallow zone due to backscatter and reflections. We consider the measurements to be unreliable above 40 Hz. The deep zone (100% water saturation) measurements are much more reliable and exhibit the frequency dependent decay consistent with the Voigt model.

## Measurement of SH-Wave Velocity Dispersion

Figure 5 shows measurements of SH-body-wave dispersion for the shallow (A) and deep (B) zones described above. Note that no significant dispersion (compared to error bars) is detectable in the dry soil (shallow zone). The deeper zone does, however, exhibit significant dispersion. This is consistent with the frequency dependant attenuation coefficient and appears to be due to the presence of water. We conclude that the water saturated deep zone behaves like a Voigt solid, and the dry shallow zone does not. Thus, we selected the deep data for a joint inversion of decay and dispersion, resulting in a solution for  $C_1$  and  $C_2$ . For a discussion of inversion theory, see Menke (1989).

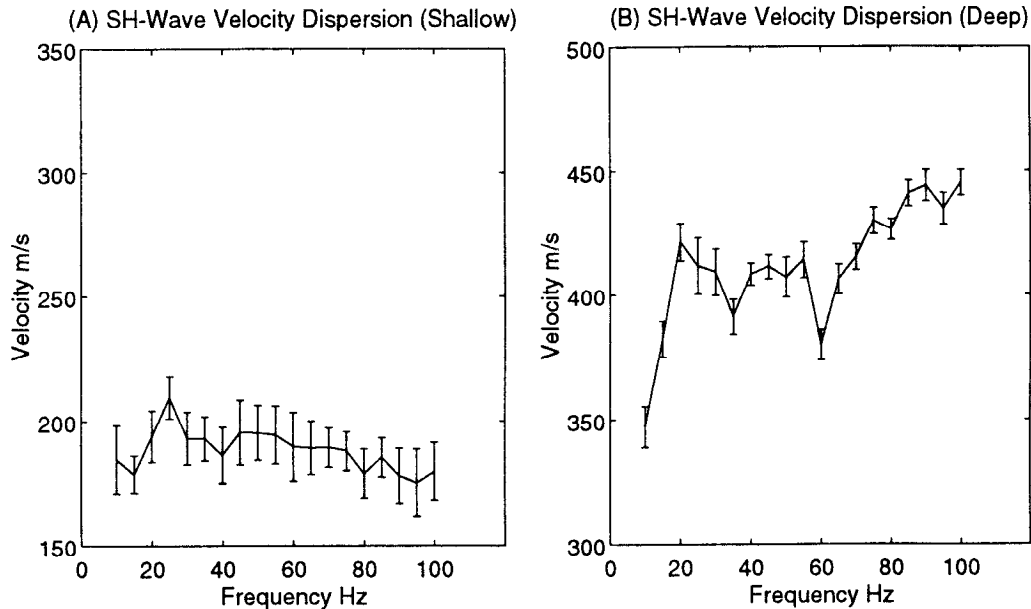


**Figure 5.** Measurements of body wave dispersion for SH-waves in the shallow, (A), and deep, (B), zones (see text). The partially saturated shallow zone, (A), exhibits no significant dispersion over this frequency range. This is at odds with a Voigt solid considering the high attenuation coefficients exhibited in Figure 4 (at least over the reliable range extending from 10 to 40 Hz). On the other hand, the fully saturated soils, (B), exhibit significant body wave dispersion. This dispersion is consistent with a Voigt solid. For that reason, only the deep zone data were inverted under the Voigt model.

### Joint Inversion

The iterative, least squares, damped inversion result is shown in Figure 6. Only the best data, from 20 to 100 Hz, were included in the inversion. The measured data are shown with circles. The computed decay and phase velocity are plotted as solid lines from the solution for  $C_1=160000 \text{ m}^2/\text{s}^2$  and  $C_2=140 \text{ m}^2/\text{s}$ . In this matrix inversion, the rows were weighted by the measurement error bars. Equal weighting was given to the decay and phase velocity measurements. The solution was achieved in only 15 iterations, and converged quite rapidly. It appears that the Voigt solid model works well, and that the combined inversion of decay and dispersion leads to two frequency invariant wave equation coefficients,  $C_1$  and  $C_2$  which predict the frequency dependent behavior of both amplitude decay and dispersion.

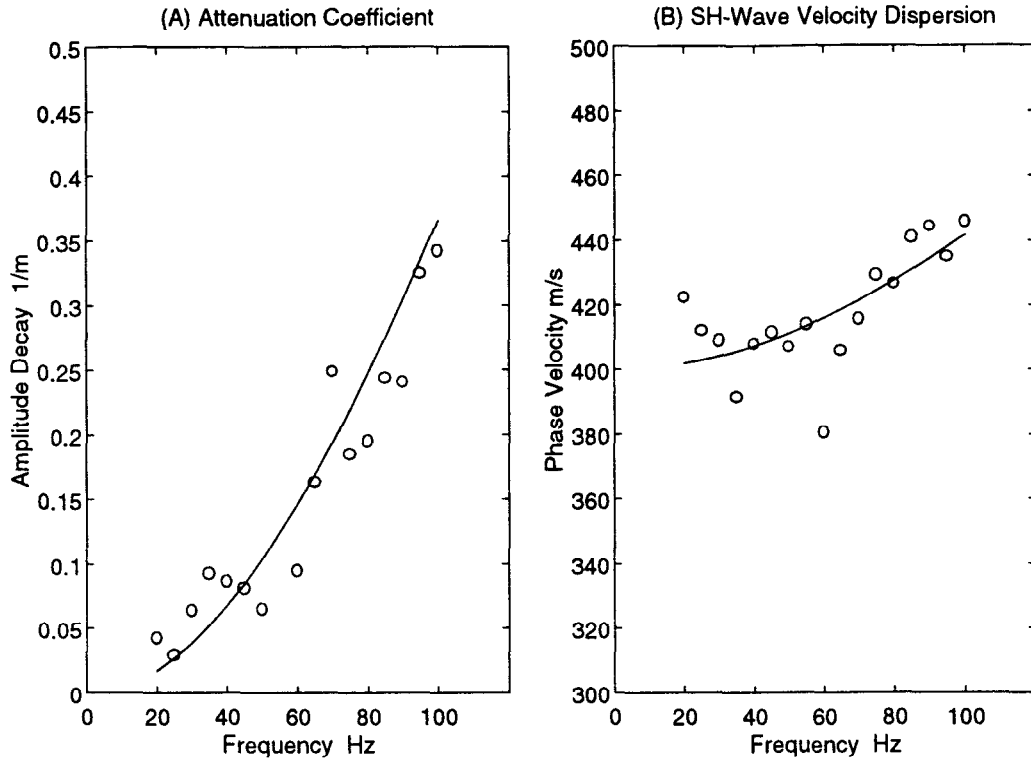


**Figure 6.** Deep zone (100% water saturated) joint inversion results showing attenuation coefficient, (A), and SH-wave velocity dispersion, (B). The measured quantities are plotted with "o" symbols and are also shown in figures 4 and 5. The computed attenuation and dispersion are plotted as solid lines for the wave equation coefficient solution  $C_1=160000 \text{ m}^2/\text{s}^2$  and  $C_2=140 \text{ m}^2/\text{s}$  (stiffness and damping respectively).

## CONCLUSIONS

We have found the following to be true at this site:

1. SH-wave velocities appear to exhibit anomalous, Type II behavior in a shallow, coarse grained, highly permeable aquifer.
2. Below the water table, the SH-wave propagation appears to be consistent with a viscous fluid (Voigt solid) model in which friction is proportional to particle velocity.
3. Above the water table, a different relaxation model seems to dominate the loss mechanism, since body wave dispersion was negligible despite a large amplitude decay factor.

Given that much of engineering practice in soil dynamics relies on a Voigt solid model, we find support for continuing that approach, provided the soil is fully saturated. More work is needed to determine what relaxation model best represents dry and partially saturated soils.

## ACKNOWLEDGMENTS

The borehole data were acquired with support from the Idaho State Board of Education Specific Research Grant A-037 and by grant DAAH04-94-G-0271 from the U.S. Army Research Office. Views and conclusions contained herein are those of the authors and should not be interpreted as necessarily representing the official policies or endorsements, either expressed or implied, of the Army Research Office or the U.S. Government. We appreciate access to the field site and operational data which have been provided by S-Sixteen Inc. and Anderson Associates Inc. CGISS contribution number 0059.

## REFERENCES AND ADDITIONAL READINGS

- Biot, M. A., 1956, Theory of propagation of elastic waves in a fluid-saturated porous solid. I Low-frequency range. *Journal of Acoust. Soc. of America*, vol. 28, no. 2, p. 168-178.
- Biot, M. A., 1962, Generalized theory of acoustic propagation in porous dissipative media: *Journal of Acoust. Soc. of America*, vol. 34, no. 9, p. 1254-1264.
- Domenico, N., 1995, Poisson's ratio -- an interdisciplinary link?: *The Leading Edge*, September, p. 983-986.
- Domenico, N., 1977, Elastic properties of unconsolidated porous sand reservoirs: *Geophysics*, vol. 42, no. 7, p. 1339-1368.
- Gregory, A.R., 1976, Fluid saturation effects on dynamic elastic properties of sedimentary rocks: *Geophysics*, vol. 41, no. 5, p. 895-921.
- Gretener, P., 1994, Reflections on the Keck visiting professorship at the Colorado School of Mines and the interdisciplinary dialog, Appendix A- The enigma of Poisson's ratio: a candidate for IDD: *The Leading Edge*, October, p. 1022-1026.
- Gajo, A., 1995, Influence of viscous coupling in propagation of elastic waves in saturated soil: *Journal of Geotechnical Engineering*, vol. 121, no. 9, p. 636-644.
- Menke, W., 1989, *Geophysical data analysis: Discrete inverse theory*, Academic Press, San Diego, Ca. 289 pgs.